MOLECULAR AND CELLULAR BIOLOGY, Nov. 2005, p. 9897–9909 Vol. 25, No. 22
0270-7306/05/$08.00+0 doi:10.1128/MCB.25.22.9897–9909.2005

Human c-Myc Isoforms Differentially Regulate Cell Growth and Apoptosis in *Drosophila melanogaster*

C. Benassayag,[1] L. Montero,[2]† N. Colombié,[1,3] P. Gallant,[2] D. Cribbs,[1] and D. Morello[1]*

Centre de Biologie du Développement, CNRS UMR 5547, Université Paul Sabatier, 118 Rte. de Narbonne, 31062 Toulouse Cedex, France[1]; Zoologisches Institut, Universität Zürich, Winterthurerstrasse 190, 8057 Zürich, Switzerland[2]; and Institut de Sciences et Technologies du Médicament de Toulouse, UMR 2587, CNRS-Pierre Fabre, 3 rue des Satellites, 31400 Toulouse, France[3]

Received 28 February 2005/Returned for modification 8 April 2005/Accepted 15 July 2005

The human c-*myc* proto-oncogene, implicated in the control of many cellular processes including cell growth and apoptosis, encodes three isoforms which differ in their N-terminal region. The functions of these isoforms have never been addressed in vivo. Here, we used *Drosophila melanogaster* to examine their functions in a fully integrated system. First, we established that the human c-Myc protein can rescue lethal mutations of the *Drosophila myc* ortholog, *dmyc*, demonstrating the biological relevance of this model. Then, we characterized a new lethal *dmyc* insertion allele, which permits expression of human c-Myc in place of dMyc and used it to compare physiological activities of these isoforms in whole-organism rescue, transcription, cell growth, and apoptosis. These isoforms differ both quantitatively and qualitatively. Most remarkably, while the small c-MycS form truncated for much of its N-terminal *trans*-activation domain efficiently rescued viability and cell growth, it did not induce detectable programmed cell death. Our data indicate that the main functional difference between c-Myc isoforms resides in their apoptotic properties and that the N-terminal region, containing the conserved MbI motif, is decisive in governing the choice between growth and death.

The Myc family of proteins, originally identified because of their cancer-inducing capacity in vertebrates, represents important and conserved regulators of cell processes including growth, proliferation, and apoptosis (21). Myc proteins are transcription factors possessing a basic helix-loop-helix leucine zipper (bHLH-LZ) and act as heterodimers in either activating or repressing transcription. Activation involves direct binding of dimers formed between Myc and its bHLH-LZ partner Max to target DNA sequences containing the E box CACGTG motif (2, 5, 35, 50). Myc can repress transcription, acting through association with Max or other protein partners such as Miz-1 to prevent binding of the basal transcriptional machinery to Inr elements (36, 47, 52; for a review, see references 9 and 21). In mammals, three related Myc genes (c-*myc*, N-*myc*, and L-*myc*) encode structurally related bHLH-LZ proteins whose overexpression is associated with tumor induction (20, 21, 30, 45). Moreover, in human, murine, and avian cells, the c-*myc* gene encodes three distinct c-Myc protein isoforms: Myc1, Myc2 (27), and a substantially shorter form called MycS (25, 55). These three isoforms are translated from distinct initiation sites, a noncanonical CUG codon for c-Myc1, an AUG located 15 codons downstream for c-Myc2 (25, 27), and an AUG 100 codons further downstream for c-MycS, respectively (55). The resulting proteins contain the same carboxy-terminal domain, including the bHLH-LZ motif, but differ in their N-terminal regions. In particular, compared to c-Myc2, c-Myc1 harbors a short N-terminal extension while the c-MycS isoform lacks the first 100 amino acids (aa) of the transactivation domain, including the well-conserved Myc box I (MbI) motif (55).

Several reports based on cell culture experiments suggest that these alternative isoforms are functionally distinct. The major variants c-Myc1 and c-Myc2 possess different *trans*-activation strengths and specificities towards the noncanonical CCAAT/enhancer-binding protein binding site; moreover, overexpression of c-Myc1, unlike that of c-Myc2, inhibits the growth of COS cells (25, 26, 35). Furthermore, these isoforms appear to be differentially regulated during cell growth, since the c-Myc2 protein is predominant in growing cells while c-Myc1 is preferred as cells approach high-density growth arrest (28). By contrast, the accumulation of c-MycS in vertebrate cells is transient during cell growth (55). Although this truncated isoform has been suggested to act as a dominant-negative inhibitor of *trans* activation by c-Myc1 and c-Myc2 proteins (55), it retains the ability to stimulate proliferation, transform Rat1a fibroblasts, induce apoptosis under low-serum conditions, and restore normal growth in Myc-null fibroblasts (57). Finally, full-length c-Myc and c-MycS show differential activities when assayed in primary versus immortalized cells, pointing to the importance of cellular background (31). Taken together, these observations show the complexity of Myc action and underline the need to directly compare the respective functions of the three isoforms in vivo. Such a study in the mouse model is complicated both by the functional redundancy of murine *myc* genes (38) and the complexity of their transcriptional and posttranscriptional regulation (39).

Drosophila melanogaster represents a good model to analyze the functions of the different human c-Myc isoforms in vivo for several reasons. The *Drosophila* genome contains a single *myc* gene, *dmyc*, which can be considered homologous to mammalian c-*myc*, based on its sequence conservation (19, 53) and the

* Corresponding author. Mailing address: Centre de Biologie du Développement, CNRS UMR 5547, Université Paul Sabatier, 118 Rte. de Narbonne, 31062 Toulouse Cedex, France. Phone: (33) 561 55 64 73. Fax: (33) 561 55 65 07. E-mail: morello@cict.fr.

† Present address: Gema Biotech S.A., Marcelo T. de Alvear 2289 1122, Buenos Aires, Argentina.

ability of dMyc protein to restore proliferation to c-Myc-deficient mouse embryonic fibroblasts (56). In addition, several *dmyc* mutations have been described in *Drosophila*, and their functional analyses reveal that dMyc protein regulates the same cellular processes as c-Myc in mammals: cell growth, proliferation and apoptosis (4, 13, 14, 34, 37, 42, 48, 51). Finally, a recently isolated lethal P insertion mutation of *dmyc* that expresses the yeast Gal4 transcriptional activator in the place of dMyc (6) allowed us to express human c-Myc1, c-Myc2, or c-MycS in place of the endogenous fly protein and directly compare their respective functions.

Here we show that each human c-Myc isoform rescues lethal *dmyc* mutations in *Drosophila melanogaster*, indicating that the fruit fly is a relevant model for studying and comparing c-Myc isoform functions in vivo. This comparison reveals markedly different isoform activities both at the level of the whole organism for rescue and at the cellular level for induction of proliferation and apoptosis. Strikingly, the transactivation domain-deleted c-MycS form rescues viability and normal proliferation but is unable to induce apoptosis. The results of this analysis, comparing the cellular activities of the three c-Myc isoforms in a physiological context, indicate a crucial role of the N-terminal region in modulating c-Myc activities in cell growth and apoptosis.

MATERIALS AND METHODS

***Drosophila* stocks.** Flies were maintained on standard corn meal-agar media at 22°C unless indicated. The *y w* line used as a control contains the isogenized X chromosome used to generate the lethal P insertions (6). Other stocks are described below.

Plasmid and transgene constructions. To construct the Myc1-encoding plasmid, RNA was extracted from the spleen of H-2/myc14 transgenic mice (49), which express the human c-Myc1 protein but not c-Myc 2 (due to an ATG-to-ATC mutation (see Fig. 2B). This RNA was reverse transcribed and amplified with forward primer 5′ GGAATTCCTTAGACGATGGATTTTTTTCGG GTAG and reverse primer 5′ GGGGTACCCCTTACGCACAAGAGTTCC G 3′ to generate the c-Myc1 PCR fragment. Subsequently, the noncanonical CTG codon was mutated to ATG to ensure its efficient translation initiation (see Fig. 2A and B). For Myc2- and MycS-encoding plasmids, total RNA was extracted from the human 293 cells, reverse transcribed, and amplified using either 5′ GGAATTCCAGCCTCCCGCGACGATGCC 3′ or 5′ GGAATTCCACGG CCGACCAGCTGGAG 3′ as forward primers and 5′ GGGGTACCCCTT ACGCACAAGAGTTCCG 3′ as the reverse primer. The 1,336-bp fragment contains the coding sequences of human c-Myc2 protein, which is translated at the canonical ATG initiation codon (see Fig. 2A). The 1,039-bp PCR fragment harbors the coding sequence for c-MycS, translated from an ATG codon located approximately 100 amino acids downstream from the ATG codon used to initiate the translation of c-Myc2 protein (25, 49). These fragments were subcloned into pGEMT Easy Vector (Promega) to generate pGEM c-Myc1, c-Myc2, and plasmids and sequenced. Their coding capacity was verified by subcloning each cDNA into the pEGFP-N3 vector downstream of the cytomegalovirus promoter (Clontech). 293 cells were transiently transfected using FuGENE 6 reagent (Roche). Proteins extracted from transfected cells were visualized using the 9E10 anti-Myc monoclonal antibody in Western blot analysis. These cDNAs were then placed under the control of upstream activation sequence (UAS) regulatory elements by subcloning them into the pUAST vector (Invitrogen) or pCaSpeR-hs (Flybase). Resulting UAS–c-Myc or heat shock protein 70 (hsp70)–c-Myc plasmids were microinjected, and multiple independent transgenic flies (≥4) were isolated for each. To obtain two copies of the c-MycS transgene, we recombined two UAS–c-MycS transgenes on chromosome 2 or 3. To ensure that these transgenic lines expressed the expected isoform, ubiquitous embryonic expression of human c-Myc isoforms was induced by crossing two independent, homozygous-viable UAS lines per isoform with a homozygous *da*-Gal4 driver line ubiquitously expressing Gal4 under *daughterless* control. Proteins extracted from ~100 *da*-Gal4>UAS–c-Myc embryos using Freon to remove yolk proteins (16) were quantified using Bio-Rad DC (detergent-compatible) protein assay, and 20 μg of each extract was submitted to Western blot analysis. c-Myc isoforms were detected using 9E10 anti-Myc monoclonal antibody. The membrane was subsequently controlled for identical protein loading using an anti-actin monoclonal antibody (Chemicon).

Characterization of new *dmyc* alleles and genetic rescue. The $dmyc^{PL35}$ and $dmyc^{PG45}$ insertions were maintained in heterogygous females, in combination with a green fluorescent protein (GFP)-expressing "Green Balancer" chromosome: FM7, B *Kr*-Gal4 UAS–GFP (KrGFP) (7). Mutant male larvae could thus be identified by the absence of fluorescence. To examine the effects of *dmyc* mutants on growth, wing disks stained with a combination of phalloidin (cytoplasmic) and chromomycin (nuclear) markers were examined by confocal microscopy. The total surface of the disk was measured. In parallel, relative cell size was estimated by counting the number of cells within two arbitrarily defined areas, one in the presumptive wing pouch and one in the notum.

Rescue of $dmyc^{PL35}$ and $dmyc^{PG45}$ insertions was initially performed using hsp70-dMyc or hsp70–c-Myc lines. Progeny were subjected to a 37°C heat shock for 1 h each day until pupal formation. For rescue experiments based on Gal4 expression, heterozygous *y w* $dmyc^{PG45}$/*FM7*, B females were crossed with lines homozygous for a UAS-dMyc or UAS–c-Myc transgene. At least two independent UAS lines were tested for each isoform. Rescue was tabulated based on eclosing B^+ males, i.e., $dmyc^{PG45}$ males rescued by expression of transgenically supplied Myc.

Rescued $dmyc^{PG45}$/*Y*; UAS–c-MycS/+ males are viable and fertile. This allowed us to test the nature of $dmyc^{PG45}$ and $dmyc^{PL35}$ by standard genetic criteria, crossing rescued males with females heterozygous for $dMyc^{PL35}$ or $dMyc^{PG45}$ or for a deficiency of the region [Df(1)75e19, 3C11;3E4;5E, and Df(1)N8, 3C1;3D6]. Female B^+ progeny obtained were of genotype $dmyc^{PG45}$/$dmyc^{PL35}$; UAS–c-MycS/+, $dmyc^{PG45}$/$dmyc^{PG45}$; UAS–c-MycS/+, or $dmyc^{PG45}$/*Df*; UAS–c-MycS/+. Rescued adult females homozygous or hemizygous for $dmyc^{PG45}$ showed a reproducible cleft between the two hemithoraces. Rescued $dmyc^{PG45}$/$dmyc^{PL35}$ *trans*-heterozygotes showed an ameliorated phenotype compared with rescued $dmyc^{PG45}$ homozygotes, confirming that $dmyc^{PL35}$ is hypomorphic. Thus, $dmyc^{PG45}$ is a strong loss-of-function allele by both formal genetic and molecular criteria.

Mitotic recombination and clonal rescue. Mitotic clones were generated by FLP/FRT-mediated site-specific recombination (58). The $dmyc^{PL35}$ and $dmyc^{PG45}$ mutants isolated as lethal P insertions of the X chromosome (6) were recombined with a Ub-GFP element on an X chromosome harboring a recombinase target site at cytological locus 18A (*dmyc* Ub-GFP FRT^{18A}). The same was also done with an arm-*lacZ* cytological marker (*dmyc* arm-*lacZ* FRT^{18A}). Clones of Ub-GFP-marked *dmyc* mutant cells were generated by crossing *dMyc* Ub-GFP FRT^{18A}/FM7, B females with arm-*lacZ* FRT18A; hsFlp MKRS/TM6B, Tb males; conversely, for arm-*lacZ*-marked *dmyc* mutant clones, crosses employed *dmyc* arm-*lacZ* FRT^{18A}/FM7, B females and Ub-GFP FRT18A; hsFlp (86E) MKRS/TM6B, Tb males. Larvae of the progeny were heat shocked for 2 h at 37.5°C at 48 and 72 h after egg deposition. Mutant clones and wild-type sister clones were identified among the unrecombined sister cells by immunostaining them with a polyclonal antibody against β-galactosidase, which permits the distinction of one or two doses of arm-*lacZ* expression, and GFP fluorescence, which likewise distinguishes one from two Ub-GFP copies. All viable cells in resulting twin spot clones were thus positively marked.

To examine cell growth rescue in *dmyc* mutant cells by human c-Myc2 and c-MycS isoforms, $dmyc^{PG45}$ arm-*lacZ* FRT^{18A}/FM7; UAS–c-Myc/+ females were crossed with Ub-GFP FRT^{18A}; C765hsFlp/TM6B Tb males. Two heat shocks (2 h at 37.5°C) were performed at 48 and 72 h of development. At the end of L3 (~120 h), Tb^+ female larvae harboring an hsFlp source were fixed, treated with anti-*lacZ* antibody, and then dissected individually; their imaginal disks were examined for the presence of mitotic clones. For genotyping, larvae were individually dissected, and their imaginal disks were mounted. Four different classes were found in the expected proportions corresponding to the following genotypes: class 1, one-fourth are FM7, *B*/Ub-GFP FRT^{18A}; class 2, one-fourth are FM7, *B*/Ub–GFP FRT^{18A}; UAS–c-Myc/+; class 3, one-fourth are $dmyc^{PG45}$ arm-*lacZ* FRT^{18A}/Ub-GFP FRT^{18A}; and class 4, one-fourth are $dmyc^{PG45}$ arm-*lacZ* FRT^{18A}/Ub-GFP FRT^{18A}; UAS–c-Myc/+. Larvae of classes 1 and 2 do not harbor mitotic clones. Class 3 larvae show a high frequency of twin spots, with the mutant spot consistently much reduced as shown in Fig. 1E. Class 4 larvae are distinguishable from class 3 larvae by the presence of twin spots with modified relative sizes.

RNA extraction and reverse transcription-PCR (RT-PCR). Total RNAs were extracted from 10 larvae or ~100 embryos by the Trizol procedure following the manufacturer's instructions (Gibco BRL). One to 2 μg of total RNA was reverse transcribed using Superscript II RNase H^- reverse transcriptase (Gibco BRL) and oligo(dT) primer in a final reaction volume of 20 μl. Semiquantitative PCR was performed using 0.5 μl of reverse transcript sample per reaction mixture,

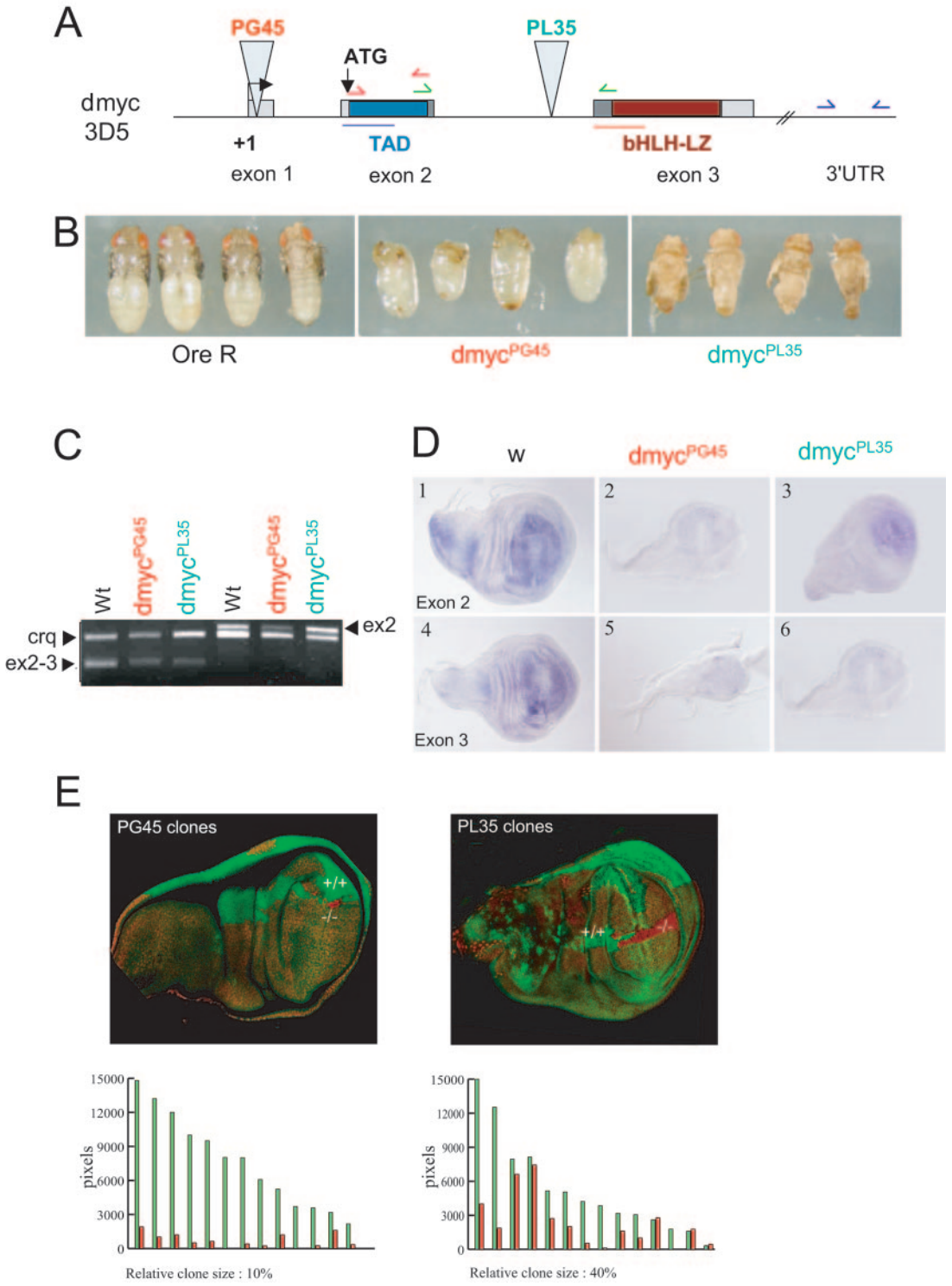

FIG. 1. Characterization of lethal *dmyc* alleles $dmyc^{PG45}$ and $dmyc^{PL35}$. (A) Structure of *dmyc*, with three exons shown. The two lethal P insertion mutations interrupt *dmyc* near the 5′ extremity and in the second intron, respectively. Primer couples used for RT-PCR are indicated as arrows above exons 2 and 3 and in the 3′ untranslated region (3′UTR). Riboprobes used for in situ hybridizations are indicated as lines under the exons. (B) Freshly eclosed wild-type Oregon R adults (OreR) are compared with dead early pupae for $dmyc^{PG45}$ or dissected pharate adults for $dmyc^{PL35}$. (C) Transcripts from wild-type and mutant *dmyc*. RNA from whole wild-type (Wt) or mutant larvae was subjected to RT-PCR, using primer couples specific for exon 2 (red) or exon 2 and 3 (green), shown in panel A. *crq* mRNA served as an internal control. Shown are the results corresponding to cycle 23. (D) *dmyc* mRNA was analyzed by in situ hybridization. Wing imaginal disks from normal (w) or mutant late L3 larvae were examined using probes specific for exon 2 (D1, D2, and D3) or exon 3 (D4, D5, and D6). (E) Clonal twin-spot analysis shows the effect of $dmyc^{PG45}$ and $dmyc^{PL35}$ on growth. Examples of typical clones are shown, with +/+ cells seen in green and −/− cells in red. The histograms show a representative spectrum of clones measuring growth of wild-type (+/+, green bars) and mutant (−/−, red bars) clones by their surface areas. $dmyc^{PG45}$ mutant clones were about 10% the size of the wild type, while for $dmyc^{PL35}$, this value was 40%.

TABLE 1. Developmental and cellular analysis of *dmyc* insertions

Genotype	% Unhatched embryos[a]	Days of pupal formation at 25°C	Lethal phase	Cell size in wing disk (pixels/cell)	Rescue of *dmyc*$^-$ males by hsp70:dMyc
Control y w	11	6	Old age	625	
PL35	11	8	Pharate adults	440	Viable adults
PG45	23	10	Prepharate pupae	411	Pharate adults

[a] The value for embryos reflects the sum of all genotypes; at later developmental phases, only mutants (GFP$^-$) were considered.

200 nM each primer, and 2 U of *Taq* polymerase (Promega). The thermal cycling conditions included an initial denaturation step (95°C for 5 min) and 20, 23, 26, or 29 cycles (each cycle consisted of 94°C for 30 s, 58°C for 30 s, and 72° for 1 min). Experiments were performed in duplicate. The sequences of the different primers used were as follows: crq (F), 5′ GCTGGCTGGAGGCACCTATCC 3′; crq (R), 5′ GCGGGAACATGTCGCCCGTGG 3′; dmyc 275 (3′/Ex2, F), 5′ CCGACGACCGGCTCTGATAG 3′; dmyc 276 (5′/Ex3,R), 5′ GGCACG AGGGATTTGTGGGTA 3′; or dmyc 277 (5′/Ex2, F), 5′ CGGCGATGTCCA GCTGTTTG 3′ and dmyc 278 (3′/Ex2, R), 5′ CGTCGGCGGAGAATCCAC TG 3′. For the autoregulation experiment, specific amplification of endogenous *dmyc* mRNA was performed using NV3 (F) (5′ GTTGGACGACGCGAAGAT GAAAGAG 3′) and NV7 (R) (5′ GGCGGCGTACTTAAAGAAATGTAT AAGG 3′) specific to sequences which are absent from the 3′ untranslated region of the transgene. The control used corresponds to *RP49* mRNA amplification using NV1 (F) and NV2 (R) primers (5′ AGATCGTGAAGAAGCGCA CCAAGC 3′ and 5′ GCACCAGGAACTTCTTGAATCCGG 3′, respectively).

In situ hybridization and immunocytology. Third-instar mutant larvae were sorted by the absence of GFP fluorescence (FM7 "Green Balancer") and then carefully staged. RNA in situ hybridizations were carried out using digoxigenin-labeled RNA probes. Immunostainings were carried out by standard procedures. The antibodies and dilutions used were as follows: rabbit anti β-galactosidase (1/5,000; Cappel), mouse anti-digoxigenin (1/2,000), rabbit anti-caspase 3, cleaved form (1/300; Cell Signaling Technology).

Flip-out clones. Females of genotype *y w* hsFlp; act>CD2>Gal4 UAS-GFP/TM6B, Tb were crossed with males homozygous for a UAS-Myc transgene and the offspring were raised at 25°C. At 48 h after egg deposition, the offspring were subjected to a 3-h heat shock in an air incubator at 37°C.

Flow cytometry. Fluorescence-activated cell sorting (FACS) analysis of wing imaginal disks harboring flip-out clones was performed as previously described (43). Wing imaginal disks were isolated from up to 25 wandering larvae and incubated for 4 to 5 h at 25° in 250 μl of phosphate-buffered saline containing 4.5-μg/μl porcine trypsin–0.18-μg/μl EDTA–0.81% NaCl (Intergen) and 0.5-ng/μl Hoechst 33342. Analysis was carried out with a FACStar PLUS (Becton Dickinson), and the data were analyzed with WinMDI, version 2.8. Each genotype was analyzed in at least two biologically independent experiments with qualitatively identical results.

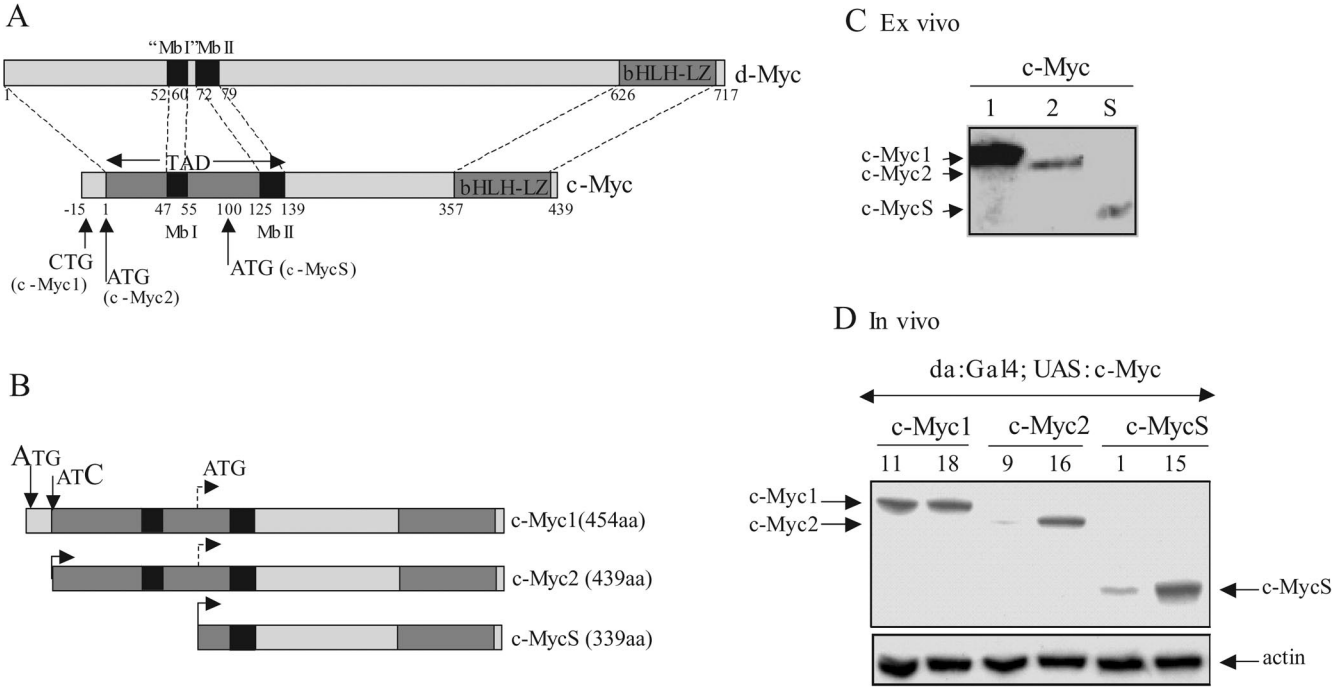

FIG. 2. Structure and expression of c-Myc proteins. (A) Block diagrams compare *Drosophila* Myc protein (d-Myc) with human c-Myc, highlighting the bHLH-LZ domain of each protein, the c-Myc *trans*-activation domain (TAD) with its MbI and MbII motifs, and the related dMyc sequences. Numbering of amino acid residues is indicated. For c-Myc, this is based on the c-Myc2 isoform (initiated at +1). Overall, the dMyc and c-Myc sequences show 26% identity (19). The bHLH-LZ region involved in DNA binding and dimerization shows extensive identity (67%; 53 of 80 residues). Three different c-Myc translation initiation codons (CTG at −15, ATG at +1, and ATG at +100) give rise to c-Myc1, c-Myc2, and c-MycS isoforms. (B) c-Myc transgenic constructs. For the c-Myc1 construction, the noncanonical CTG codon was modified to ATG, while the alternate downstream ATG site was changed to ATC to limit initiation site choice. c-Myc2 and c-MycS constructs employed the usual ATG codons. (C) Proteins extracted from transiently transfected culture cells were subjected to Western blot analysis and detected with anti-Myc monoclonal antibody. A single band of the expected size was detected for each construct. (D) Proteins extracted from *da*-Gal4>UAS–c-Myc embryos were analyzed as described for panel C. Two independent transgenic lines were tested for c-Myc1, c-Myc2, and c-MycS. As for transfected cells, a single protein band of the predicted size was seen for each construct.

TABLE 2. Transgenic rescue of the *dmyc*^{PG45} mutant

dmyc^{PG-45}/FM7 × UAS-transgenic lines (*n*)	Rescued males *dmyc*^{PG45}/Y; UAS-Myc						Myc-overexpressing females *dmyc*^{PG45}/+; UAS-Myc		
	% Viability[a]			Phenotype	% Wing size[b] (*n* = 40)	% Cell size[c]	% Viability[d]		
	18°C (*n* = 30)	22°C (*n* = 70)	26°C (*n* = 70)				18°C (*n* = 80)	22°C (*n* = 150)	26°C (*n* = 120)
UAS-dMyc (3)	0	0	0				30 (±5)	3 (±2)	0
UAS–c-Myc1 (6)	0	0	0				52 (±6)	41 (±1)	3 (±3)
UAS–c-Myc2 (4)	66 (±25)	30 (±15)	0	Normal bristles; sterile	90	93	>100	66 (±3)	38 (±3)
UAS–c-MycS (6)	28 (±3)	40 (±2)	20 (±2)	Thin bristles; fertile	85	83	>100	>100	78 (±3)
2 copies UAS–c-MycS (2)	>100	85 (±5)	55 (±5)	Thin bristles; fertile	ND	ND	>100	>100	>100

[a] Relative to FM7/Y males; *n*, number of males counted.
[b] Relative to wings of *y w*/Y males; *n*, number of wings counted.
[c] Relative to cell size of *y w*/Y male wings (see Materials and Methods).
[d] Relative to FM7/+; UAS-Myc females; *n*, number of females counted. ND, not determined.

RESULTS

Characterization of lethal *dmyc* insertions. In a recent systematic genetic screen for P element insertions that interrupt essential genes on the *Drosophila* X chromosome, we isolated two new *dmyc* insertions (PG45 and PL35), both associated with recessive lethality (6). The PG45 (an enhancer trap expressing the Gal4 reporter gene) and PL35 (expressing *lacZ*) lines are integrated adjacent to the putative *dmyc* transcription start site and in the second intron, respectively (Fig. 1A). Mutant males harboring either allele die throughout larval-pupal development, with a delayed development compared to that of wild-type controls (Table 1).

While a majority of PG45 male larvae die early in the pupal stage, PL35 males die later, as pharate pupae of reduced size with

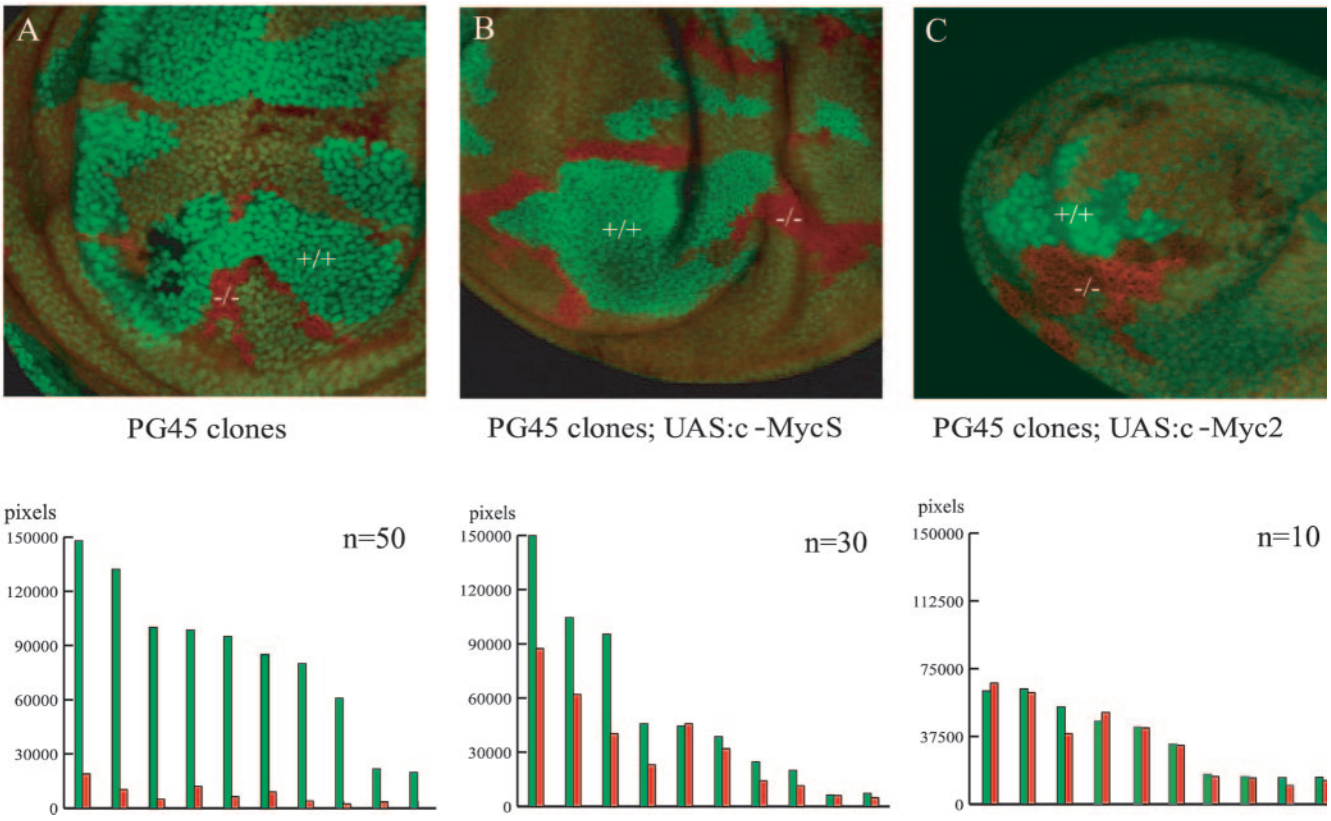

FIG. 3. Rescue of growth by c-Myc proteins in *dmyc* mutant cells. Representative clones were examined for +/+ (green) or *dmyc*^{PG45}/*dmyc*^{PG45} (red) cells without c-Myc (A), expressing c-MycS (B), or c-Myc2 (C) from UAS constructs under *dmyc*^{PG45} control as described in the text. At bottom, a histogram summarizing the results from representative clones (*n* = number of clones analyzed) shows that human c-Myc restored cell growth to about 70% and 100% of wild-type levels for cells expressing c-MycS and c-Myc2, respectively. Note that for mutant cells expressing c-Myc2, the frequency of clones observed per disk was markedly reduced compared with clones of cells expressing c-MycS or for mutant cells alone.

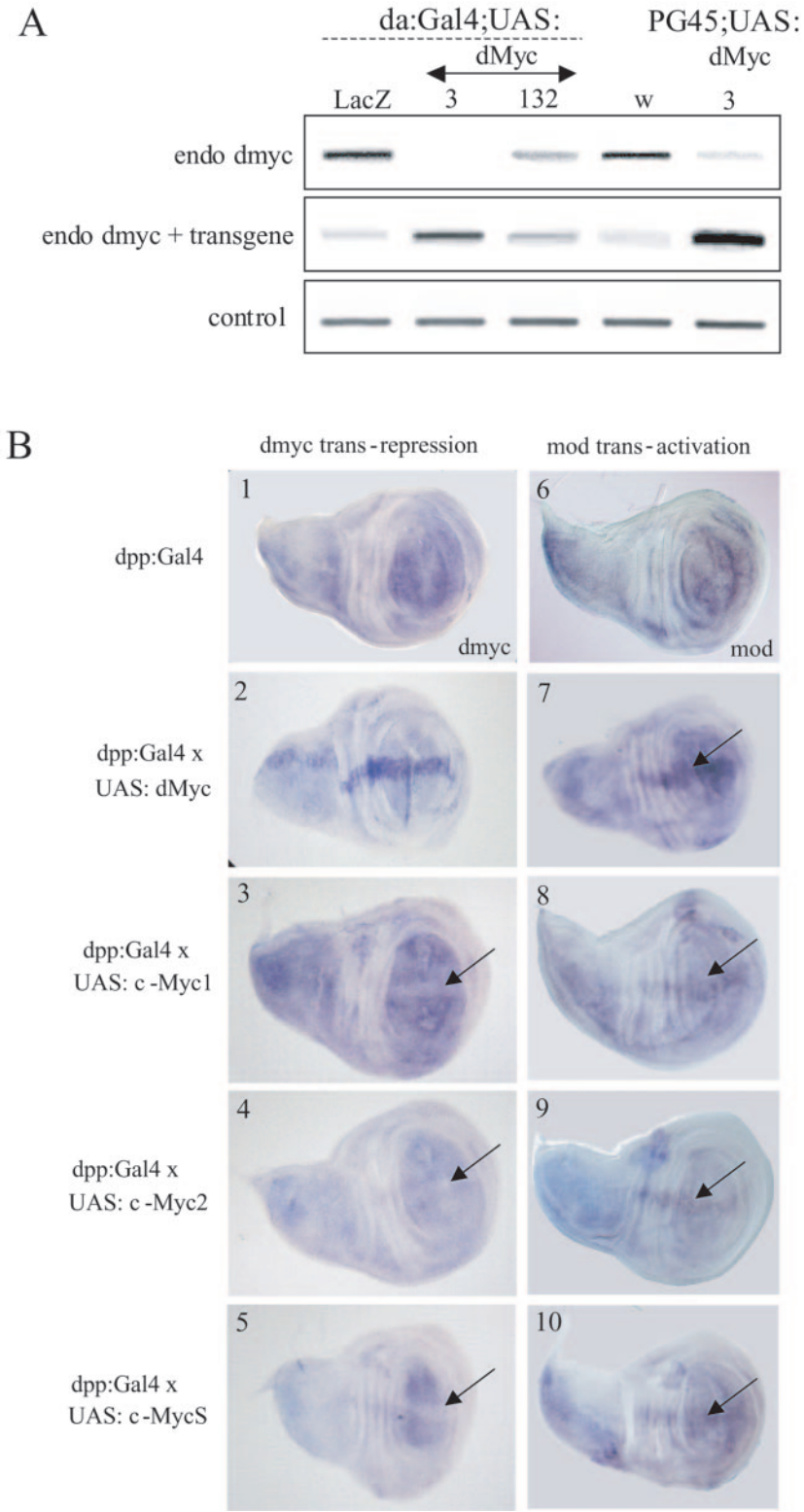

FIG. 4. Human c-Myc isoforms regulate dMyc target genes. (A) Negative autoregulation of *dmyc*. RT-PCR was carried out with RNAs extracted from embryos carrying *da*-Gal4 and a UAS transgene directing the expression of LacZ or dMyc (lines 3 and 132), or from wild type (w) or selected $dmyc^{PG45}$; UAS-dMyc (line 3) larvae. Primer pairs (Fig. 1A and Materials and Methods) specifically amplified mRNAs from endogenous *dmyc* (endo), both endogenous and transgenic *dmyc* (endo dmyc plus transgene) or RP49 (control). Shown are the results corresponding to cycle 26 (endo), 23 (endo plus transgene) and 20 (RP49). (B) The imaginal disk-specific *dpp*-Gal4 driver was used to direct localized overexpression of Myc forms from UAS constructs, in a central band of cells in otherwise wild-type wing imaginal disks (as seen for *dmyc* in B2). The effect on transcription from *dmyc* (panels 1 to 5) or *mod* (panels 6 to 10) was detected by in situ hybridization to wing imaginal disks, using

a thin bristle phenotype similar to that of previously described *dmyc* alleles (Fig. 1B) (34). Heterozygous females are viable, fertile, develop at a normal rate, and appear morphologically normal as adults, showing that both insertions are recessive.

The lethality of PL35 and PG45 males can be attributed to the P element insertions in *dmyc* for three reasons. First, lethality can be fully reverted by transposase-induced precise excision (6; data not shown). Second, both insertions are associated with strongly reduced levels of *dmyc* mRNA in third-instar male larvae, as assessed by semiquantitative RT-PCR using different combinations of primers (Fig. 1C) and by in situ hybridization to wing imaginal disks with exon-specific probes (Fig. 1D). Whereas *dmyc* mRNA is normally expressed at high levels in the wing pouch but is excluded from cells flanking the dorsoventral boundary (Fig. 1D1 and 4) (19), only background levels of *dmyc* mRNA were detected throughout the PG45 mutant disks for all probes tested (Fig. 1D2 and 5). In PL35 larvae, hybridization revealed accumulation of a truncated mRNA containing exon 2 but not exon 3 (Fig. 1D3 and 6), which was confirmed by RT-PCR with appropriate primers (Fig. 1C). Third, the lethality of PL35 and PG45 mutants can be rescued by expression of a dMyc transgene (Table 1) (32). Taken together, the mutant phenotype, *dmyc* mRNA expression and transgenic rescue confirm that these insertions are indeed *dmyc* loss-of-function mutations (that we refer to as $dmyc^{PL35}$ and $dmyc^{PG45}$) with $dmyc^{PG45}$ being the stronger of the two.

$dmyc^{PL35}$ and $dmyc^{PG45}$ insertions affect cell growth. It has previously been shown that *dmyc* mutant cells grow poorly compared to the wild type, as measured in vivo in a mitotic recombination-cell competition assay (34). To estimate the strength of the new, lethal *dmyc* alleles, we first compared relative numbers and sizes of cells in wing imaginal disks of staged *dmyc* mutant late third-instar larvae compared to the wild type (see Materials and Methods). Total wing disk size was reduced by ~30% for both mutants (Fig. 1D), and the mutant cell area was also one-third smaller than that of the wild type (Table 1). The similar reductions in the sizes of cells, imaginal disks (Fig. 1D), and pupae (23 to 30% smaller in mutants) (Fig. 1B) indicate that cell size is the primary determinant of organ size. Next, we used the FLP/FRT system to induce site-specific mitotic recombination in female larvae heterozygous for $dmyc^{PG45}$ or $dmyc^{PL35}$, and quantitated the relative growth of normal and mutant cells by measuring the area of +/+ (green) and $dmyc^{-}$/$dmyc^{-}$ (red) cell clones. Both $dmyc^{PG45}$ and $dmyc^{PL35}$ mutant clones grew poorly compared to their sister clones (Fig. 1E). While the relative size of $dmyc^{PL35}$ mutant clones varied considerably, from 0% to 100% of the wild-type twin (average relative size, 40%) (Fig. 1E), the effect on cell growth was invariably strong for $dmyc^{PG45}$, with an average mutant clone size of about 10% of the wild-type twin (Fig. 1E). These data show that $dmyc^{PG45}$ strongly affects cell growth and, taken together with the above molecular characterization and formal genetic analysis (see Materials and Methods), confirm that $dmyc^{PG45}$ is a strong hypomorphic allele (37).

Human c-Myc isoforms differentially rescue lethal *dmyc* mutations. To test whether human c-Myc can replace dMyc function in vivo, we examined $dmyc^{PG45}$ and $dmyc^{PL35}$ mutant males harboring hsp70–c-Myc transgenes (see Materials and Methods and below). The lethal phase for $dmyc^{PG45}$ males was retarded on inducing c-Myc1 or c-Myc2 expression (or for dMyc [Table 1]), while a few mutant $dmyc^{PL35}$ adult males survived. This result demonstrated a rescue capacity, but the multiple heat shocks required were associated with widely variable viability and limited rescue. We therefore focused on the $dmyc^{PG45}$ insertion, which not only removes normal gene function but also expresses the Gal4 activator protein in a pattern very similar to normal *dmyc* expression (data not shown). The Gal4 activator protein was used to activate transcription of the various UAS–c-Myc constructs through their UAS sequences.

The human c-Myc coding sequences were modified such that the noncanonical CUG codon in c-Myc1 was replaced by an AUG and the downstream AUG from which c-Myc2 translation is normally initiated was replaced by AUC (Fig. 2B and Materials and Methods). Each cDNA directed the accumulation of a single protein when transiently transfected in 293 cultured cells (Fig. 2C). We established at least four independent UAS–c-Myc transgenic fly lines for each cDNA. To verify expression of the appropriate c-Myc isoform in vivo, two independent UAS lines for each isoform were crossed with a driver line ubiquitously expressing Gal4 under *daughterless* control (*da*–Gal4) and proteins extracted from the resulting embryos. In each case, Western blot analysis showed the predicted c-Myc isoform (Fig. 2D).

We next coupled UAS–Myc transgenes with the $dmyc^{PG45}$ mutation to test the ability of the three c-Myc isoforms to rescue $dmyc^{PG45}$ mutant males. Such males were obtained by crossing females heterozygous for $dmyc^{PG45}$ with males homozygous for each UAS–c-Myc insertion (at least four independent lines). Since Gal4 activity is enhanced by increasing temperature, expression levels for Myc proteins were modulated by raising cultures in parallel at 18°C, 22°C, or 26°C. The $dmyc^{PG45}$ insertion is fully lethal in hemizygous males, and thus recovery of adult $dmyc^{PG45}$ males will demonstrate that the transgenic Myc protein has compensated the loss of normal *dmyc* function. Such males were observed on expressing either c-MycS or c-Myc2 (Table 2), showing that despite poor overall conservation, human c-Myc can rescue the loss of dMyc function in vivo.

However, the three c-Myc proteins tested were not equivalent in this rescue assay. Indeed, rescued mutant males expressing c-MycS were viable and fertile for the six single-insertion lines tested and for two recombinant lines carrying two insertion copies, whereas surviving c-Myc2 expressing males were sterile (four lines tested) (Table 2). In stark contrast, no c-Myc1-expressing males were obtained for any line or growth

specific riboprobes (exon 2 for *dmyc* and full-length cDNA for *mod*). Endogenous *dmyc* and *mod* expression is shown in panels 1 and 6, respectively, while patterns resulting from overexpressed Myc forms are shown for dMyc line 3 (panels 2 and 7), c-Myc1 line 18 (panels 3 and 8), c-Myc2 line 16 (panels 4 and 9) or c-MycS line 15 (panels 5 and 10). All c-Myc forms detectably repressed *dmyc* (left, arrows) and enhanced expression of *mod* (right, arrows) in a central band of cells.

condition tested (Table 2). This discrepancy is not due to differences in expression level, since protein isoform accumulation was similar for independent transgenic lines expressing c-Myc1, c-Myc2, and c-MycS (Fig. 2D, compare Myc1-11 and -18 and Myc2-16 and MycS-15). The absence of rescue for c-Myc1 (comparable to the dMyc control) (Table 2) may thus reflect a dominant toxicity of this isoform under these expression conditions. This hypothesis is supported by the marked effect of increasing culture temperature on survival of c-Myc1-expressing $dmyc^{PG45}$/+ female progeny (52% survival at 18°C versus 3% at 26°C) (Table 2) or to a lesser extent for c-Myc2 (100% at 18°C versus 38% at 26°C) (Table 2). By contrast, c-MycS-expressing females were fully represented at any temperature, and addition of a second transgenic copy in mutant males improved rescue efficiency (Table 2). Taken together, these data suggest that human c-Myc isoforms differ qualitatively in their action and notably that c-MycS—described as a transactivation-deficient, dominant negative c-Myc form (57)—can efficiently replace dMyc in vivo.

Human c-Myc isoforms restore *Drosophila* cell growth. These rescue data strongly suggest that the various c-Myc proteins are not functionally equivalent in the whole organism. To better understand these differences, we examined the capacities of c-Myc2 and c-MycS to restore cellular growth in vivo. Due to the dominant lethality associated with expression from UAS-dMyc or UAS–c-Myc1, these forms could not be tested. We made use of the FLP/FRT site-specific recombination system to induce mitotic recombination in females heterozygous for $dmyc^{PG45}$ and harboring a UAS–c-Myc transgene. Mitotic recombination yielded twin recombinant clones of +/+; UAS–c-Myc and mutant $dmyc^{PG45}/dmyc^{PG45}$; UAS–c-Myc cells, with the former cells expressing only endogenous *dmyc* and the mutant cells expressing transgenic c-Myc. In the absence of c-Myc protein, the size of the mutant clone (red) was strongly reduced compared to the (green) wild-type twin spot (10%) (Fig. 1E and 3A). By contrast, growth rescue was observed in clones of cells expressing either c-MycS or 2. This cellular rescue appeared nearly complete for the c-Myc2-expressing clones (Fig. 3C), while c-MycS-expressing clones were about 70% the size of the +/+ twin (Fig. 3B). Similarly, c-Myc2-rescued adults attained nearly normal size, while c-MycS-expressing adults were smaller by about 15%, as seen by wing size (Table 2). We conclude that human c-Myc2 and c-MycS differentially substitute for endogenous *dmyc* in promoting cell growth and that the sizes of the resulting adults reflect different cellular growth properties of these c-Myc isoforms.

Human c-Myc isoforms regulate dMyc target genes. The functional rescue of *dmyc* mutations by c-Myc suggests that human and *Drosophila* Myc proteins control common target genes in vivo. To address this question, we examined the capacity of c-Myc isoforms to regulate known or potential *dmyc* targets in flies. c-*myc* expression in mammals is subject to a negative autoregulatory loop (17). To test whether a similar regulatory mechanism exists in *Drosophila*, we overexpressed transgenic dMyc and measured its effect on accumulation of endogenous *dmyc* mRNA. The endogenous and transgenic *dmyc* mRNAs differ in their 3′ untranslated regions, making it possible to specifically detect the endogenous mRNA by RT-PCR (Materials and Methods). As shown in Fig. 4A, endogenous *dmyc* expression was strongly reduced upon UAS-dMyc expression directed either by *da*-Gal4 or by $dmyc^{PG45}$ drivers (endo *dmyc*). This repression was inversely related to the level of transgene expression (Fig. 4A, compare transgenic lines 3 versus 132). These data indicate the existence of a negative autoregulatory mechanism conserved between mammals and flies.

We next asked whether the different human c-Myc isoforms can *trans* repress *dmyc* transcription, using the *dpp*-Gal4 driver to direct their localized expression in a central band of cells at the anteroposterior compartment boundary of wing imaginal disks. We then examined *dmyc* mRNA accumulation by in situ hybridization with a *dmyc*-specific exon 2 riboprobe (Fig. 1A). The control experiment with UAS-dMyc showed a strong localized accumulation of *dmyc* mRNA, as expected for the *dpp* promoter used (Fig. 4B2). In contrast, when human c-Myc forms were expressed in the same manner, endogenous *dmyc* mRNA was locally diminished (compare Fig. 4B1 to 4B3 to 5, arrows). These observations indicate that all three human c-Myc proteins can negatively regulate *dmyc*.

We next examined their capacity to *trans* activate the expression of two known *dmyc* target genes, *pitchoune* (*pit*) and *modulo* (*mod*). *pit* encodes an RNA helicase required for cell growth (60), while the Modulo protein shows structural similarity to nucleolin, which has a putative role in ribosome biogenesis (46). Expression of either *pit* or *mod* is strongly reduced in $dmyc^{PG45}$ or $dmyc^{PL35}$ mutants (46; data not shown). To ask whether human Myc proteins can activate transcription of these genes, we induced dMyc or isoform specific c-Myc expression in the wing imaginal disk and then analyzed *pit* and *mod* expression by in situ hybridization. Locally enhanced expression for *mod* (Fig. 4B7, arrow) or *pit* (not shown) was induced by dMyc, compared with endogenous expression (Fig. 4B6 and data not shown); similar, albeit weaker, enhancement was observed with all three human c-Myc variants (Fig. 4B8 to 10). Taken together, we conclude that fly and human Myc proteins are able to regulate the same target genes, whether negatively (*dmyc) or* positively (*pit* and *mod*).

Human c-Myc isoforms differentially modulate cell growth and cell cycle progression. We next sought to compare the activities of the three c-Myc isoforms for cellular functions in vivo, i.e., cell growth, cell cycle progression, and apoptosis, by examining the effects of their overexpression in a wild type context. We therefore generated random clones of cells overexpressing c-Myc1, c-Myc2, or c-MycS in imaginal wing disks under the control of Gal4 by the flip-out technique (act>CD2>Gal4; Materials and Methods) (43). Clones of Gal4-expressing cells induced during larval development were identified by cytoplasmic GFP expression from a UAS:GFP reporter. Such GFP^+ cells were then separated from nonexpressing cells by FACS, and both populations were examined for cell size and DNA content. Expression of dMyc, used in a control experiment, led to an increase in cell size (Fig. 5, left) and a strong reduction in the fraction of cells in G_1 with a concomitant increase in cells in S or G_2 phase (Fig. 5, right), as previously described (34). Human isoforms c-Myc1 and 2 produced similar effects, albeit weaker than for dMyc (Fig. 5). However, c-MycS, while promoting G_1/S cell cycle progression, had little effect on cell size (Fig. 5). To test whether this difference might reflect limiting amounts of c-MycS activity, we induced flip-out clones expressing two UAS–c-MycS copies

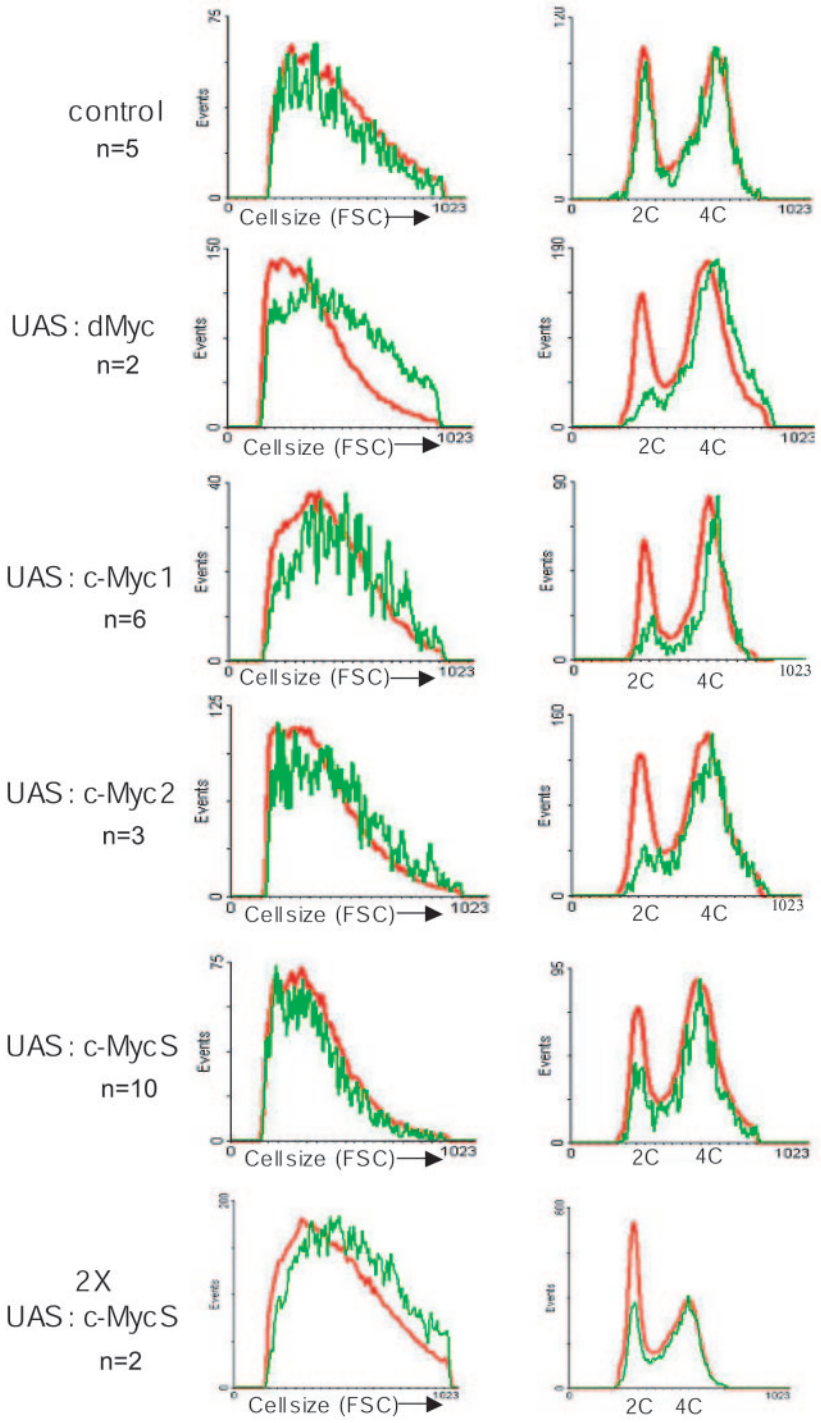

FIG. 5. Effects of Myc overexpression on cell size and cell cycle distribution. Flip-out clones of cells expressing Gal4 were generated by FLP recombinase derived from an hsFlp construct by heat induction 2 days after egg laying. Corresponding wing disks in third-instar larvae were dissected 3 days later. Clonally derived cells expressing Myc proteins (UAS-Myc transgene) were identified by coexpression of the GFP marker from a UAS-GFP transgene. Shown are representative FACS analyses of dissociated wing disk cells. (Left) Cellular size was assayed by forward scatter (FSC). (Right) Cell cycle distribution was assessed by measuring accumulation of the DNA-intercalating dye Hoechst 33342. The vertical axis indicates cell number; red traces correspond to control cells expressing neither GFP nor the Myc transgene; green traces correspond to cells from the same wing disks but expressing the indicated Myc transgene together with GFP. To standardize the presentations, we set the 4C peak of each green trace to the same level as the 4C peak of the corresponding red trace. The apparent overrepresentation of the 2C peak for the red control curve observed in the right bottom panel reflects variation among experiments but is not isoform specific. To ensure the reliability of results obtained from small cell numbers, the experiments were repeated several times (*n*).

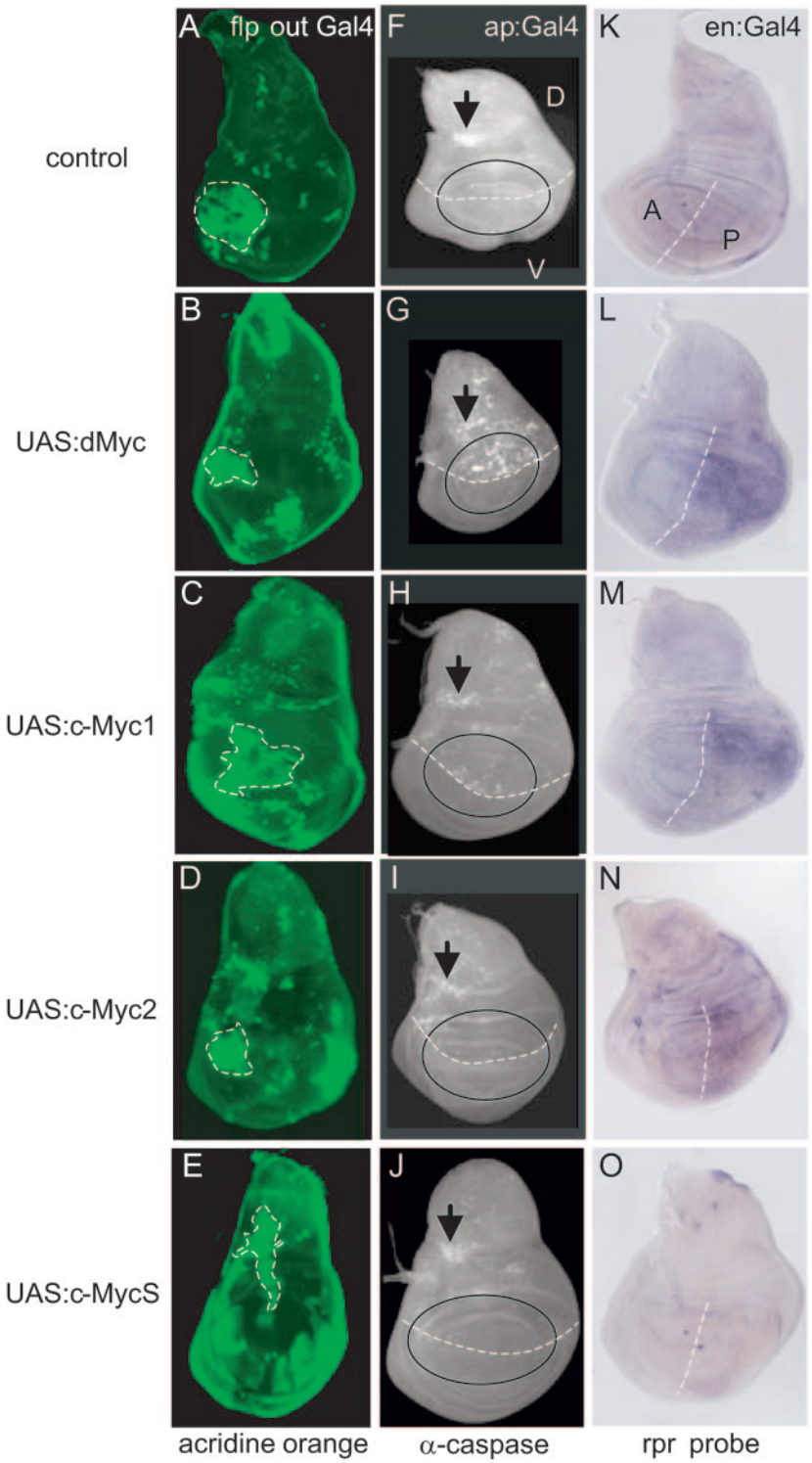

FIG. 6. Effects of overexpressing Myc forms on apoptosis and *reaper* gene expression. (Left) Immunofluorescence micrographs of intact wing disks harboring flip-out clones of cells expressing the indicated transgenes in clones. The clones are recognized by their diffuse, evenly distributed green staining (corresponding to UAS-GFP expression; examples are indicated by dotted lines). Bright green dots correspond to AO staining typical of apoptotic cells. Intense AO staining was observed in clones of cells expressing dMyc (B) and c-Myc1 (C); lesser AO staining was seen for c-Myc2-expressing cells (D), while apoptotic cells accumulating AO were not observed in control clones (A) or in clones expressing c-MycS (E). (Middle) UAS-Myc transgenes were expressed in the dorsal compartment of wing imaginal disks under the control of *ap*-Gal4, and apoptosis was detected by an antibody directed against activated caspase 3 (G to J). The approximate dorsoventral compartment boundary is indicated in each image by a broken line, while the wing pouch is roughly delimited by an oval. The consequences of Myc expression are seen in the dorsal half of the wing pouch (roughly corresponding to the upper half of the area marked by the oval). Whereas dMyc and c-Myc1 provoked strong apoptosis (G and H), c-Myc2 and c-MycS samples (I and J) were similar to the *lacZ* control (F). Consistently high background levels of apoptosis independent

rather than one. Under these conditions, the effect of c-MycS on cell size-cell cycle progression resembled that of c-Myc1 and c-Myc2 (Fig. 5).

Human c-Myc isoforms have different effects on apoptosis. To ask whether Myc overexpression induces apoptosis, we examined the uptake of the vital stain acridine orange (AO) (1) in imaginal disks harboring Myc-expressing flip-out clones (GFP^+). Apoptotic cells show intense nuclear staining with this dye. High levels of apoptosis were observed within clones of cells expressing dMyc, c-Myc1, or c-Myc2 (compare Fig. 6B to D to Fig. 6A). In striking contrast, c-MycS did not induce detectable apoptosis with one or two transgenic UAS–c-MycS copies (Fig. 6E and data not shown). Similar results were obtained with another experimental condition, where an *ap*-Gal4 driver was used to express c-Myc isoforms in dorsal wing disk cells (wing pouch and notum), and apoptosis was visualized with an antibody directed against activated caspase 3, a marker for apoptotic cells (40). Significant background levels of localized apoptosis, presumably due to the *ap*-Gal4 insertion, were observed outside the wing pouch for all samples (Fig. 6F to J, arrows). However, strong additional apoptosis in dorsal cells of the wing pouch was specifically observed on overexpressing dMyc and c-Myc1 (compare Fig. 6G and H to the control, shown in Fig. 6F). In contrast, c-Myc2 showed (at most) modest induction (Fig. 6I), while none was noted for c-MycS (Fig. 6J). This result confirms that c-Myc isoforms can differentially induce apoptosis: strongly for c-Myc1, weakly for c-Myc2, and none for c-MycS. We therefore next asked whether the differential induction of apoptosis could reflect different abilities of the human isoforms to activate the pro-apoptotic *reaper* (*rpr*) gene, recently identified as a dMyc target by a genome-wide search and shown to be up-regulated by dMyc in vivo (14, 44). To this end, an independent driver line, *engrailed*-Gal4, was used to direct Myc expression in posterior cells of wing imaginal disks during larval development, and *rpr* mRNA expression was examined by in situ hybridization. As seen in Fig. 6L and M, posterior *rpr* mRNA expression was markedly induced by dMyc and c-Myc1, and to a lesser extent by c-Myc2 (Fig. 6N). However, only background levels of *rpr* mRNA were observed upon c-MycS expression using one or two copies of the transgene (Fig. 6O and not shown). Together, these data indicate that the inability of the c-MycS isoform to induce apoptosis in vivo is at least in part due to its inability to activate *rpr* transcription.

DISCUSSION

In the present work, we have compared the capacity of the three human c-Myc isoforms to rescue lethal *dmyc* mutations, modulate cell growth, and induce apoptosis in *Drosophila*. All three isoforms, but especially c-Myc2 and c-MycS, are capable of restoring viability in *dmyc* mutants and of regulating dMyc target genes in vivo. Thus, despite limited sequence identity, fly and human Myc proteins are functionally conserved and deploy a common network during *Drosophila* development. However, the rescue experiments and clonal analysis also revealed marked functional distinctions among human c-Myc forms in their ability to induce cell growth or programmed cell death. Strikingly, the transactivation domain-truncated c-MycS isoform efficiently rescues fly viability and fertility when expressed in place of dMyc but induces no detectable apoptosis in overexpression conditions in vivo. Our findings support the interpretation that promoting cell growth-proliferation and inducing apoptosis are distinct properties of Myc proteins residing in their amino terminal regions.

Conserved Myc functions from fly to humans. Myc plays an essential role in controlling body size both in *Drosophila* and in mice. In *Drosophila*, dMyc is thought to promote cell growth (23, 34), while in mice, Myc appears to regulate both cell proliferation (56) and growth (3, 13, 22, 33). Previous observations showed that proliferation defects of c-Myc-deficient embryonic fibroblasts can be partially alleviated by dMyc expression (56). The whole-organism rescue of lethal *dmyc* mutations by c-Myc expression presented here demonstrates that human and *Drosophila* Myc proteins retain sufficiently similar cellular functions to sustain a normal, integrated development. Accordingly, we have shown that they regulate common target genes involved in cell growth and apoptosis (*dmyc*, *pitchoune*, *modulo*, and *reaper*). This ability of c-Myc to successfully replace dMyc in transcription is particularly striking in light of the poor conservation of their N-terminal regions, including the transactivation domain. For example, full identity is observed in the region containing MbI motifs from mammalian, bird, frog, and fish c-Myc proteins (18), whereas fly dMyc MbI is highly divergent (19). The success of highly diverged mammalian c-Myc in regulating developmental processes in the fly suggests that their regulatory networks are remarkably conserved.

Isoform-specific c-Myc functions. The preceding results confirm that flies constitute a relevant physiological model for the detailed comparison of the cellular and molecular properties distinguishing c-Myc isoforms. To this end, we used the lethal $dmyc^{PG45}$ allele that expresses the transcription activator Gal4 in place of dMyc. When expressed under $dmyc^{PG45}$ control, dMyc and c-Myc1 were unable to rescue mutants, apparently due to a dominant toxicity, even at low levels of expression (18°C). c-Myc2 can restore viability but might also be toxic when expressed at higher levels (26°C). In marked contrast, c-MycS efficiently rescued males, even at elevated expression levels (two transgene copies at 26°C) (Table 2). We can exclude that this contrasting behavior reflects differential isoform accumulation due to different protein stabilities or expression levels because (i) the functionally distinct c-Myc1 and c-Myc2 isoforms accumulated similarly as detected by Western blotting

of Myc activity (F to J, arrows) are presumably due to the *ap*-Gal4 insertion. (Right) Effects of Myc overexpression on *reaper* (*rpr*) expression (K to O). UAS-Myc transgenes were expressed in the posterior compartment of wing imaginal disks under *en*-Gal4 control, and *rpr* gene expression was visualized by in situ hybridization. The approximate anteroposterior compartment boundary is indicated by the line in all panels (K to O). Clear induction of *rpr* expression in the wing pouch was observed for dMyc and c-Myc1 (L and M), while weaker induction was detected for c-Myc2 (N). c-MycS did not induce detectable *rpr* expression (compare panels K and O). The wing imaginal disks depicted are representative and were photographed at the same magnification.

(Fig. 2D) and (ii) for a given isoform, multiple independent lines tested gave similar results in all functional tests (Table 2), even when their expression levels varied (cf. c-Myc2 and c-MycS) (Fig. 2D). We therefore infer that the functional differences of c-Myc isoforms observed in the physiological context of *Drosophila* development primarily reflect their distinct molecular and cellular properties.

From several previous analyses of cultured cells, it was already suggested that the three c-Myc isoforms behave differently in controlling cell growth, proliferation, and apoptosis (10, 31, 54, 55, 57). Here, we reexamined isoform-specific cellular roles in the physiological context of the whole organism where c-Myc can replace endogenous dMyc. Under these conditions, we have found that c-Myc forms can be distinguished by both quantitative and qualitative traits. All three modulate cell size and cell cycle progression when overexpressed; however, they showed unequal efficiencies, since higher doses of c-MycS were required for an equivalent effect on cell size (Fig. 5). In agreement with this observation, c-MycS expressed in *dmyc* mutant cells restored growth less fully than c-Myc2 (Fig. 3). Concerning their capacities to induce apoptosis, however, c-Myc isoforms show clear differences. Cells expressing c-Myc1 showed high levels of apoptosis comparable to dMyc. By contrast, the effect of c-Myc2 was much milder and c-MycS had no discernible effect, even at levels sufficient to increase cell size (two transgene copies) (Fig. 6 and data not shown).

Taken together, our data argue that of the three human c-Myc isoforms, c-Myc1 is functionally comparable to dMyc. Relative to c-Myc1, the c-Myc2 isoform is similarly competent in inducing cell growth but attenuated for apoptosis, while c-MycS lacking another 100 aa of its N-terminal region conserves an ability to stimulate cell growth but has lost proapoptotic function. However, c-MycS is able to fully rescue *dmyc* mutants, suggesting that proapoptotic activity is not required for normal development. Conversely, the strong induction of apoptosis by c-Myc1 compared to c-Myc2 (Fig. 6) might explain their differential toxicity in the developing fly.

The growth-versus-death choice is influenced by the c-Myc N terminus. At the level of the primary amino acid sequence, the only difference between the predominant vertebrate form c-Myc2 and alternative c-Myc1 and c-MycS forms resides in their NH_2 terminal portion (Fig. 2A). In *dmyc* mutant *Drosophila*, the cellular functions of c-Myc2 are sufficient to sustain normal development. Remarkably, the alternatively initiated c-Myc1, which harbors an additional 15 aa, enhanced all these cellular functions and (in particular) apoptosis but led to dominant lethality. This optional, leucine-initiated sequence is relatively weakly conserved between the closely related human and mouse proteins (6 identical amino acids out of 15). The *Drosophila dmyc* locus also possesses an in-frame leucine codon 15 aa upstream of the presumptive ATG initiation site. If translated as in vertebrates, the resulting 15-aa sequence would not be conserved (1 of 15 identical amino acids in the three species). The poor overall conservation of this sequence argues against its specific interaction with molecular partners and suggests an indirect role favoring a productive conformation of c-Myc protein.

The N-terminal region common to c-Myc1 and c-Myc2 contains a *trans*-activation domain that has been described as important for numerous properties of the Myc molecule and/or for its interactions with molecular partners in cultured cells (12, 21). In the *trans*-activation domain, MbI is believed to play a role in modulating c-Myc activity, while the integrity of MbII is essential to normal c-Myc functions including cell cycle progression, apoptosis, and transformation (41). c-MycS lacks the first 100 aa, including the MbI motif, which harbors two phosphorylation sites (Thr 58 and Ser 62) involved in the stability of c-Myc protein through proteosomal degradation (15, 59). Mutations of these sites are often linked to B-cell lymphomas (24, 29) and are correlated with reduced apoptotic potential (8, 11). Curiously, neither of these sites is conserved in dMyc (19). The truncated c-MycS isoform rescues the growth defect of c-Myc null fibroblasts (57), but its ability to transactivate and induce apoptosis remains a subject of debate (31, 57). The rescue obtained on expressing c-MycS in developing *Drosophila* clearly shows that this isoform possesses all necessary properties to sustain growth and development, even though it is fully deficient in inducing apoptosis. These results thus support the possibility of a direct role for the first 100 aa of the N-terminal region, absent from c-MycS, in the cellular choice between growth or death. This choice will presumably reflect discriminating physical interactions of a given N-terminal sequence with specific cofactors. The uncoupling between growth and death functions obtained in c-MycS but not in c-Myc2 transgenic flies thus offers an exciting new opportunity to dissect the c-Myc genetic network(s) underlying these two cellular processes.

Altogether, our results obtained in a physiological context show that the three c-Myc isoforms are functionally different, with the principal characteristic distinguishing them being their abilities to induce apoptosis. In their normal context in mammalian cells, these c-Myc isoforms do not accumulate singly but in specific combinations or ratios characteristic of a given cellular status. Their different abilities to induce apoptosis may thus explain why perturbing their balance can be associated with cellular pathologies, including oncogenesis.

ACKNOWLEDGMENTS

We thank our colleagues in Toulouse for many helpful discussions and Nathalie Vanzo and Alain Vincent for their critical readings of the text. *en*- and *ap*-Gal4 driver lines and UAS-*lacZ* and UAS-GFP responder lines were obtained from the Indiana University *Drosophila* Stock Center. cDNAs for *modulo* and *pitchoune* were generously provided by Laurent Perrin and Michel Semeriva, while Michèle Crozatier kindly provided the cDNA for *reaper*. We thank Agnès Lepage for her expert technical assistance, Henri Dupont for his crucial assistance with Western blot analysis, Bruno Savelli and Brice Ronsin for their help with the confocal microscope and the preparation of figures, and Eva Niederer for help with the FACS analysis.

This work benefited from the ongoing support of the Centre National de Recherche Scientifique (CNRS) and from grants from the Swiss Cancer League (SKL) and SNF (to P.G.), from the Université Paul Sabatier (BQR) (to D.C. and D.M.), and from the Association pour la Recherche sur le Cancer (ARC) (to D.M.).

REFERENCES

1. **Abrams, J. M., K. White, L. I. Fessler, and H. Steller.** 1993. Programmed cell death during Drosophila embryogenesis. Development **117:**29–43.
2. **Amati, B., S. Dalton, M. W. Brooks, T. D. Littlewood, G. I. Evan, and H. Land.** 1992. Transcriptional activation by the human c-Myc oncoprotein in yeast requires interaction with Max. Nature **359:**423–426.
3. **Arabi, A., S. Wu, K. Ridderstrale, H. Bierhoff, C. Shiue, K. Fatyol, S. Fahlen, P. Hydbring, O. Soderberg, I. Grummt, L. G. Larsson, and A. P. Wright.** 2005. c-Myc associates with ribosomal DNA and activates RNA polymerase I transcription. Nat. Cell Biol. **7:**303–310.
4. **Bates, C. M., S. Kharzai, T. Erwin, J. Rossant, and L. F. Parada.** 2000. Role of N-myc in the developing mouse kidney. Dev. Biol. **222:**317–325.

5. **Blackwood, E. M., and R. N. Eisenman.** 1991. Max: a helix-loop-helix zipper protein that forms a sequence-specific DNA-binding complex with Myc. Science **251:**1211–1217.
6. **Bourbon, H. M., G. Gonzy-Treboul, F. Peronnet, M. F. Alin, C. Ardourel, C. Benassayag, D. Cribbs, J. Deutsch, P. Ferrer, M. Haenlin, J. A. Lepesant, S. Noselli, and A. Vincent.** 2002. A P-insertion screen identifying novel X-linked essential genes in Drosophila. Mech. Dev. **110:**71–83.
7. **Casso, D., F. Ramirez-Weber, and T. B. Kornberg.** 2000. GFP-tagged balancer chromosomes for Drosophila melanogaster. Mech. Dev. **91:**451–454.
8. **Chang, D. W., G. F. Claassen, S. R. Hann, and M. D. Cole.** 2000. The c-Myc transactivation domain is a direct modulator of apoptotic versus proliferative signals. Mol. Cell. Biol. **20:**4309–4319.
9. **Claassen, G. F., and S. R. Hann.** 1999. Myc-mediated transformation: the repression connection. Oncogene **18:**2925–2933.
10. **Cole, M. D.** 1986. The myc oncogene: its role in transformation and differentiation. Annu. Rev. Genet. **20:**361–384.
11. **Conzen, S. D., K. Gottlob, E. S. Kandel, P. Khanduri, A. J. Wagner, M. O'Leary, and N. Hay.** 2000. Induction of cell cycle progression and acceleration of apoptosis are two separable functions of c-Myc: transrepression correlates with acceleration of apoptosis. Mol. Cell. Biol **20:**6008–6018.
12. **Dang, C. V.** 1999. c-Myc target genes involved in cell growth, apoptosis and metabolism. Mol. Cell. Biol. **19:**1–11.
13. **de Alboran, I. M., R. C. O'Hagan, F. Gartner, B. Malynn, L. Davidson, R. Rickert, K. Rajewsky, R. A. DePinho, and F. W. Alt.** 2001. Analysis of C-MYC function in normal cells via conditional gene-targeted mutation. Immunity **14:**45–55.
14. **de la Cova, C., M. Abril, P. Bellosta, P. Gallant, and L. A. Johnston.** 2004. Drosophila myc regulates organ size by inducing cell competition. Cell **117:** 107–116.
15. **Dominguez-Sola, D., and R. Dalla-Favera.** 2004. PINning down the c-Myc oncoprotein. Nat. Cell Biol. **6:**288–289.
16. **Evans, J. P., and B. K. Kay.** 1991. Biochemical fractionation of oocytes. Methods Cell Biol. **36:**133–148.
17. **Facchini, L. M., S. Chen, W. W. Marhin, J. N. Lear, and L. Z. Penn.** 1997. The Myc negative autoregulation mechanism requires Myc-Max association and involves the c-*myc* P2 minimal promoter. Mol. Cell. Biol. **17:**100–114.
18. **Fladvad, M., K. Zhou, A. Moshref, S. Pursglove, P. Safsten, and M. Sunnerhagen.** 2005. N and C-terminal sub-regions in the c-Myc transactivation region and their joint role in creating versatility in folding and binding. J. Mol. Biol. **346:**175–189.
19. **Gallant, P., Y. Shiio, P. F. Cheng, S. M. Parkhurst, and R. N. Eisenman.** 1996. Myc and Max homologs in Drosophila. Science **274:**1523–1527.
20. **Garte, S. J.** 1993. The c-myc oncogene in tumor progression. Crit. Rev. Oncog. **4:**435–449.
21. **Grandori, C., S. M. Cowley, L. P. James, and R. N. Eisenman.** 2000. The Myc/Max/Mad network and the transcriptional control of cell behavior. Annu. Rev. Cell Dev. Biol. **16:**653–699.
22. **Grandori, C., N. Gomez-Roman, Z. A. Felton-Edkins, C. Ngouenet, D. A. Galloway, R. N. Eisenman, and R. J. White.** 2005. c-Myc binds to human ribosomal DNA and stimulates transcription of rRNA genes by RNA polymerase I. Nat. Cell Biol. **7:**311–318.
23. **Grewal, S. S., L. Li, A. Orian, R. N. Eisenman, and B. A. Edgar.** 2005. Myc-dependent regulation of ribosomal RNA synthesis during Drosophila development. Nat. Cell Biol. **7:**295–302.
24. **Gupta, S., A. Seth, and R. J. Davis.** 1993. Transactivation of gene expression by Myc is inhibited by mutation at the phosphorylation sites Thr-58 and Ser-62. Proc. Natl. Acad. Sci. USA **90:**3216–3220.
25. **Hann, S. R.** 1995. Methionine deprivation regulates the translation of functionally-distinct c-Myc proteins. Adv. Exp. Med. Biol. **375:**107–116.
26. **Hann, S. R., M. Dixit, R. C. Sears, and L. Sealy.** 1994. The alternatively initiated c-Myc proteins differentially regulate transcription through a non-canonical DNA-binding site. Genes Dev. **8:**2441–2452.
27. **Hann, S. R., M. W. King, D. L. Bentley, C. W. Anderson, and R. N. Eisenman.** 1988. A non-AUG translational initiation in c-myc exon 1 generates an N-terminally distinct protein whose synthesis is disrupted in Burkitt's lymphomas. Cell **52:**185–195.
28. **Hann, S. R., K. Sloan-Brown, and G. D. Spotts.** 1992. Translational activation of the non-AUG-initiated c-myc 1 protein at high cell densities due to methionine deprivation. Genes Dev. **6:**1229–1240.
29. **Henriksson, M., A. Bakardjiev, G. Klein, and B. Luscher.** 1993. Phosphorylation sites mapping in the N-terminal domain of c-myc modulate its transforming potential. Oncogene **8:**3199–3209.
30. **Henriksson, M., and B. Luscher.** 1996. Proteins of the Myc network: essential regulators of cell growth and differentiation. Adv. Cancer Res. **68:**109–182.
31. **Hirst, S. K., and C. Grandori.** 2000. Differential activity of conditional MYC and its variant MYC-S in human mortal fibroblasts. Oncogene **19:**5189–5197.
32. **Hulf, T., P. Bellosta, M. Furrer, D. Steiger, D. Svensson, A. Barbour, and P. Gallant.** 2005. Whole-genome analysis reveals a strong positional bias of conserved dMyc-dependent E-boxes. Mol. Cell. Biol. **25:**3401–3410.
33. **Iritani, B. M., and R. N. Eisenman.** 1999. c-Myc enhances protein synthesis and cell size during B lymphocyte development. Proc. Natl. Acad. Sci. USA **96:**13180–13185.
34. **Johnston, L. A., D. A. Prober, B. A. Edgar, R. N. Eisenman, and P. Gallant.** 1999. Drosophila myc regulates cellular growth during development. Cell **98:**779–790.
35. **Kretzner, L., E. M. Blackwood, and R. N. Eisenman.** 1992. Myc and Max proteins possess distinct transcriptional activities. Nature **359:**426–429.
36. **Li, L. H., C. Nerlov, G. Prendergast, D. MacGregor, and E. B. Ziff.** 1994. c-Myc represses transcription in vivo by a novel mechanism dependent on the initiator element and Myc box II. EMBO J. **13:**4070–4079.
37. **Maines, J. Z., L. M. Stevens, X. Tong, and D. Stein.** 2004. Drosophila dMyc is required for ovary cell growth and endoreplication. Development **131:**775–786.
38. **Malynn, B. A., I. M. de Alboran, R. C. O'Hagan, R. Bronson, L. Davidson, R. A. DePinho, and F. W. Alt.** 2000. N-myc can functionally replace c-myc in murine development, cellular growth, and differentiation. Genes Dev. **14:** 1390–1399.
39. **Marcu, K. B., S. A. Bossone, and A. J. Patel.** 1992. myc function and regulation. Annu. Rev. Biochem. **61:**809–860.
40. **Martin, S. J.** 2002. Destabilizing influences in apoptosis: sowing the seeds of IAP destruction. Cell **109:**793–796.
41. **McMahon, S. B., H. A. Van Buskirk, K. A. Dugan, T. D. Copeland, and M. D. Cole.** 1998. The novel ATM-related protein TRRAP is an essential cofactor for the c-Myc and E2F oncoproteins. Cell **94:**363–374.
42. **Moreno, E., and K. Basler.** 2004. dMyc transforms cells into super-competitors. Cell **117:**117–129.
43. **Neufeld, T. P., A. F. de la Cruz, L. A. Johnston, and B. A. Edgar.** 1998. Coordination of growth and cell division in the Drosophila wing. Cell **93:** 1183–1193.
44. **Orian, A., B. van Steensel, J. Delrow, H. J. Bussemaker, L. Li, T. Sawado, E. Williams, L. W. Loo, S. M. Cowley, C. Yost, S. Pierce, B. A. Edgar, S. M. Parkhurst, and R. N. Eisenman.** 2003. Genomic binding by the Drosophila Myc, Max, Mad/Mnt transcription factor network. Genes Dev. **17:**1101–1114.
45. **Oster, S. K., C. S. Ho, E. L. Soucie, and L. Z. Penn.** 2002. The myc oncogene: MarvelouslY complex. Adv. Cancer Res. **84:**81–154.
46. **Perrin, L., C. Benassayag, D. Morello, J. Pradel, and J. Montagne.** 2003. Modulo is a target of Myc selectively required for growth of proliferative cells in Drosophila. Mech. Dev. **120:**645–655.
47. **Peukert, K., P. Staller, A. Schneider, G. Carmichael, F. Hanel, and M. Eilers.** 1997. An alternative pathway for gene regulation by Myc. EMBO J. **16:**5672–5686.
48. **Pierce, S. B., C. Yost, J. S. Britton, L. W. Loo, E. M. Flynn, B. A. Edgar, and R. N. Eisenman.** 2004. dMyc is required for larval growth and endoreplication in Drosophila. Development **131:**2317–2327.
49. **Pistoi, S., J. Roland, C. Babinet, and D. Morello.** 1996. Exon 2-mediated c-*myc* mRNA decay in vivo is independent of its translation. Mol. Cell. Biol. **16:**5107–5116.
50. **Prendergast, G. C., D. Lawe, and E. B. Ziff.** 1991. Association of Myn, the murine homolog of max, with c-Myc stimulates methylation-sensitive DNA binding and ras cotransformation. Cell **65:**395–407.
51. **Quinn, L. M., R. A. Dickins, M. Coombe, G. R. Hime, D. D. Bowtell, and H. Richardson.** 2004. Drosophila Hfp negatively regulates dmyc and stg to inhibit cell proliferation. Development **131:**1411–1423.
52. **Roy, A. L., C. Carruthers, T. Gutjahr, and R. G. Roeder.** 1993. Direct role for Myc in transcription initiation mediated by interactions with TFII-I. Nature **365:**359–361.
53. **Schreiber-Agus, N., D. Stein, K. Chen, J. S. Goltz, L. Stevens, and R. A. DePinho.** 1997. Drosophila Myc is oncogenic in mammalian cells and plays a role in the diminutive phenotype. Proc. Natl. Acad. Sci. USA **94:**1235–1240.
54. **Spencer, C. A., and M. Groudine.** 1991. Control of c-myc regulation in normal and neoplastic cells. Adv. Cancer Res. **56:**1–48.
55. **Spotts, G. D., S. V. Patel, Q. Xiao, and S. R. Hann.** 1997. Identification of downstream-initiated c-Myc proteins which are dominant-negative inhibitors of transactivation by full-length c-Myc proteins. Mol. Cell. Biol. **17:**1459–1468.
56. **Trumpp, A., Y. Refaeli, T. Oskarsson, S. Gasser, M. Murphy, G. R. Martin, and J. M. Bishop.** 2001. c-Myc regulates mammalian body size by controlling cell number but not cell size. Nature **414:**768–773.
57. **Xiao, Q., G. Claassen, J. Shi, S. Adachi, J. Sedivy, and S. R. Hann.** 1998. Transactivation-defective c-MycS retains the ability to regulate proliferation and apoptosis. Genes Dev. **12:**3803–3808.
58. **Xu, T., and G. M. Rubin.** 1993. Analysis of genetic mosaics in developing and adult Drosophila tissues. Development **117:**1223–1237.
59. **Yada, M., S. Hatakeyama, T. Kamura, M. Nishiyama, R. Tsunematsu, H. Imaki, N. Ishida, F. Okumura, K. Nakayama, and K. I. Nakayama.** 2004. Phosphorylation-dependent degradation of c-Myc is mediated by the F-box protein Fbw7. EMBO J. **23:**2116–2125.
60. **Zaffran, S., A. Chartier, P. Gallant, M. Astier, N. Arquier, D. Doherty, D. Gratecos, and M. Semeriva.** 1998. A Drosophila RNA helicase gene, pitchoune, is required for cell growth and proliferation and is a potential target of d-Myc. Development **125:**3571–3584.